

**Reply to “Interactive comment on “The vertical variability of ammonia in urban Beijing, China” by Yangyang Zhang et al.” (Referee #1 in RC2)**

Monitoring NH<sub>3</sub> concentration in the air is an important step to validate the remote sensing data of NH column concentration and understand the emission sources for mitigation. Owing to the high cost of monitoring, long term monitoring data with a high vertical resolution is little. This paper provided such a dataset in Beijing where is suffering serious air pollution, and NH<sub>3</sub> emission is believed having a significant contribution.

Generally speaking, although the innovation on scientific question is not strong in this paper, its contribution on the understanding of NH<sub>3</sub> emission, transportation, mixture in the atmosphere is still significant through providing a long term dataset. From such a perspective, this paper is deserved publication with proper revision suggested as follow.

Re: Thank you for your valuable comments and appreciation of our study. We have made changes and corrections in the revised manuscript. We respond in detail to the questions and comments below (in blue). Actually, we had revised the manuscript as you suggested before ACPD, so we highlighted the revised parts in yellow.

Specific comments:

Line 22-24 Seasonal variation of average NH<sub>3</sub> concentration across the profile was described in the abstract; it is well-known in previous studies. Seasonal variation of vertical distribution of NH<sub>3</sub> concentration should be the point of your study. It is also true for transport analyses. Please, revise it.

Re: Thanks for this suggestion. We have updated this section to read:

The highest seasonal NH<sub>3</sub> concentrations across the profile were observed in summer (18.2 μg m<sup>-3</sup>) with high temperature, followed by spring (13.4 μg m<sup>-3</sup>), autumn (12.1 μg m<sup>-3</sup>), and winter (8.3 μg m<sup>-3</sup>). Significant vertical variation of NH<sub>3</sub> concentration was only found in summer. Source region analyses suggest that air masses from intensive agricultural regions to the south contribute most to the high

30 [NH<sub>3</sub> concentrations in Beijing.](#)

Line 42-44, NH<sub>3</sub> emission in China has been updated. Please see Zhang, X., Wu, Y., Liu, X., Reis, S., Jin, J., Dragosits, U., Van Damme, M., Clarisse, L., Whitburn, S., Coheur, P., Gu, B., 2017. Ammonia emissions may be substantially underestimated in China. Environ. Sci. Technol. 51, 12089-12096.

35 [Re: We have updated the text with the suggested reference.](#)

Line 45-51, contribution of NH<sub>3</sub> to the urban air pollution have been studied well. See follow

40 Gu, B., Sutton, M.A., Chang, J., Chang, S.X., Ge, Y., 2014. Agricultural ammonia emissions contribute to China's urban air pollution. Front. Ecol. Environ. 12, 265-266.

Wu, Y., Gu, B., Erisman, J.W., Reis, S., Fang, Y., Lu, X., Zhang, X., 2016. PM<sub>2.5</sub> pollution is substantially affected by ammonia emissions in China. Environ. Pollut. 218, 86-94.

[Re: We have added these additional references in the manuscript.](#)

45 Line 141 "75th", "th" is superscript

[Re: Thanks. The expression was corrected in the revised manuscript.](#)

Line 153 Weekly NH<sub>3</sub> concentration was low to 4.4  $\mu\text{g m}^{-3}$ , here you said almost NH<sub>3</sub> concentrations were above 5  $\mu\text{g m}^{-3}$ , please give a detailed number (how many percentage).

50 [Re: 99.6% of the weekly samples were above 5  \$\mu\text{g m}^{-3}\$ . We have added the following sentence to the text:](#)

[Nearly all \(99.6%\) of the weekly NH<sub>3</sub> concentrations along the profile exceeded 5  \$\mu\text{g m}^{-3}\$ .](#)

Line 159-163 Move the "BAO tower" results to the discussion section, they are

55 previous results, not yours.

Re: The “BAO tower” results have been moved to the discussion section.

Line 171 Does the first “autumn” should be “summer”? Check the whole manuscript and revise the relative expressions.

Re: The expressions were corrected accordingly.

60 Line 193  $\text{NH}_3(\text{g}) + \text{HNO}_3(\text{g}) \rightarrow \text{NH}_4\text{NO}_3(\text{p})$

Re: Agree and corrected.

Line 233-234 The BAO study (1985) may be too old to compare with your study (2016). Please find other comparable references.

Re: The old reference was replaced by a new one (Li et al., 2017).

65 Reference:

1. Li, Y., Thompson, T. M., Damme, M. V., Chen, X., Benedict, K. B., Shao, Y., Day, D., Boris, A., Sullivan, A. P., and Ham, J.: Temporal and spatial variability of ammonia in urban and agricultural regions of northern Colorado, United States, *Atmos. Chem. Phys.*, 17, 6197-6213, <https://doi.org/10.5194/acp-17-6197-2017>, 2017.

70

Line 271 You say twice about the surfaces can be sources or sinks. Please rephrase the whole paragraph to give a clear statement.

Re: This paragraph was rephrased in the revised manuscript. It now reads:

75 Surfaces can act either as sources or sinks of  $\text{NH}_3$ , depending on surface  $\text{NH}_3$  content, ambient  $\text{NH}_3$  concentrations, and local meteorology and surface type (Tevlin et al., 2017; Zhang et al., 2010).

Fig.2 3 replicates were performed, but where is the S.D. for  $\text{NH}_3$  concentrations?

Re: The standard deviation of the replicates (black lines) have been added in Fig.2.

80 Others: please improve the quality (readability) of Figs. E.g. how do you get the results of NH<sub>3</sub> emission distribution in fig. 1 left; do statistical analyses for all seasons in fig.3; the heights (15, 63, 120, 180, 240 and 320 m) were selected in fig.5, which are 2, 63, 180, and 320 m in fig.6, and 8, 63, 120, 180, 240 and 320 m in fig. S6, it is good to select the same height. Fig S2.

85 Re: We now state in the caption of Fig. 1 that "NH<sub>3</sub> emission estimates are from the inventory of Zhang et al. (2018) at 0.1° horizontal resolution". We also did repeated-measures analysis of variance (ANOVA) in Fig.3.

Regarding the selected heights, because of the missing temperature data for 2m and 8m, we used 15 m instead of 8 m in Fig 5; for PSCF analysis (Fig.6), 2 m was selected to reveal the local surface source.

90 Reference:

1. Zhang, L., Chen, Y., Zhao, Y., Henze, D. K., Zhu, L., Song, Y., Paulot, F., Liu, X., Pan, Y., and Lin, Y.: Agricultural ammonia emissions in China: reconciling bottom-up and top-down estimates, *Atmos. Chem. Phys.*, 18, 339-355, <https://doi.org/10.5194/acp-18-339-2018>, 2018.

95

## The vertical variability of ammonia in urban Beijing, China

Yangyang Zhang<sup>1</sup>, Aohan Tang<sup>1,\*</sup>, Dandan Wang<sup>1</sup>, Qingqing Wang<sup>2</sup>, Katie Benedict<sup>3</sup>, Lin Zhang<sup>4</sup>, Duanyang Liu<sup>5</sup>, Yi Li<sup>6</sup>, Jeffrey L. Collett Jr.<sup>3</sup>, Yele Sun<sup>2,Z\*</sup>, Xuejun Liu<sup>1,\*</sup>

<sup>1</sup>Beijing Key Laboratory of Farmland Soil Pollution Prevention and Remediation, College of Resources and Environmental Sciences, China Agricultural University, Beijing 100193, China

<sup>2</sup>State Key Laboratory of Atmospheric Boundary Layer Physics and Atmospheric Chemistry, Institute of Atmospheric Physics, Chinese Academy of Sciences, Beijing 100029, China

<sup>3</sup>Department of Atmospheric Science, Colorado State University, Fort Collins, CO80523, USA

<sup>4</sup>Laboratory for Climate and Ocean–Atmosphere Studies, Department of Atmospheric and Oceanic Sciences, School of Physics, Peking University, Beijing 100871, China

<sup>5</sup>Jiangsu Meteorological Observatory, Nanjing 210008, China

<sup>6</sup>Sunset CES Inc., Beaverton, OR97008, USA

<sup>7</sup>[Collaborative Innovation Center on Forecast and Evaluation of Meteorological Disasters, Nanjing University of Information Science & Technology, Nanjing 210044, China](#)

\*Corresponding authors (aohantang@cau.edu.cn, sunyele@mail.iap.ac.cn, liu310@cau.edu.cn)

**Abstract.** Weekly vertical profiles of ammonia (NH<sub>3</sub>) were measured at 16 heights on the Beijing 325 m meteorological tower for one year from March 2016 to March 2017. ~~Measured The~~ average NH<sub>3</sub> concentrations ~~at all heights~~ exceeded ~~5–4~~  $\mu\text{g m}^{-3}$  ~~at all heights~~ with an overall average ( $\pm 1\sigma$ ) ~~tower concentration value~~ of  $13.3 (\pm 4.8) \mu\text{g m}^{-3}$ . The highest NH<sub>3</sub> concentrations along the vertical profiles mostly occurred at 32–63 m, decreasing both towards the surface and at higher altitudes. Significant decreases in NH<sub>3</sub> concentrations were only found at the top two heights (280 and 320 m). These results suggest an ~~NH<sub>3</sub> ammonia~~ rich atmosphere during all seasons in urban Beijing, from the ground to at least 320 m. ~~Highest concentrations were observed in summer, associated with high temperature.~~ The ~~highest average seasonal~~ NH<sub>3</sub> concentrations ~~s~~ across the profile ~~were from high to low was~~ observed in summer ( $18.2 \mu\text{g m}^{-3}$ ) ~~with high temperature~~, followed by spring ( $13.4 \mu\text{g m}^{-3}$ ), autumn ( $12.1 \mu\text{g m}^{-3}$ ), and winter ( $8.3 \mu\text{g m}^{-3}$ ). ~~Significant vertical variation of NH<sub>3</sub>~~

带格式的: 到齐到网格

带格式的: 英语(英国)

带格式的: 突出显示

concentration was only found in summer. Source region Transport analyses suggest that air masses arriving from intensive agricultural regions to the south contribute most to the high NH<sub>3</sub> concentrations in Beijing. Local sources such as traffic emissions also appear to be important contributors to atmospheric NH<sub>3</sub> in this urban environment.

## 1. Introduction

Ammonia (NH<sub>3</sub>) has long been recognized as an important form of reactive nitrogen (Nr) in atmospheric environment, playing a key role in biogeochemical cycles from atmospheric chemical processes to deposition and subsequent environmental impacts (e.g. air pollution, reduced biodiversity, acidification, and eutrophication) (Fowler et al., 2009; Sutton et al., 2008). NH<sub>3</sub> reacts with nitric and sulfuric acids in air, forming secondary inorganic aerosols (e.g., NH<sub>4</sub>NO<sub>3</sub>, (NH<sub>4</sub>)<sub>2</sub>SO<sub>4</sub>) with long atmospheric lifetimes that can transport these species far from sources and contribute 40-57% of fine particle matter in megacities (Fowler et al., 2009; Huang et al., 2014; Yang et al., 2011). Therefore, NH<sub>3</sub> has received increasing attention in air pollution research (Wang et al., 2015). In addition to agriculture, which is considered the largest NH<sub>3</sub> source globally, emissions from biomass burning, industries, vehicles, and other sources (Galloway et al., 2003; Sutton et al., 2008; Erisman et al., 2008; Sun et al., 2016; Sun et al., 2017) can also be significant.

In China, annual NH<sub>3</sub> emissions were approximately 2- and 3 times higher than European and US emissions, respectively, over the period 1990 to 2005 (Reis et al., 2009; Kang et al., 2016; Zhao and Wang, 1994; Klimont, 2001; EMEP; USEPA, 2009), and estimated at 14.6 Tg N yr<sup>-1</sup> in 2010 (Liu et al., 2013) and 15.6 Tg N yr<sup>-1</sup> in 2015 (Zhang et al., 2017) (Reis et al., 2009; Kang et al., 2016; Zhao and Wang, 1994; Klimont, 2001; EMEP; USEPA, 2009; Zhang et al., 2017). Such high emissions, together with the important role NH<sub>3</sub> plays in degrading air quality, makes NH<sub>3</sub> a key target to curb serious air pollution in Chinese urban areas (Fu et al., 2017; Chang et al., 2016; Ye et al., 2011; Wang et al., 2011). Some studies have indicated that reducing NH<sub>3</sub> concentrations could be an effective method for alleviating secondary inorganic PM<sub>2.5</sub> pollution in China (Gu et al., 2014; Wang et al., 2015; Wu et al., 2016; Xu et al., 2017). However, NH<sub>3</sub> has been received less attention from the government, however, than SO<sub>2</sub> and NO<sub>x</sub>, which have been controlled since 2005 and been effectively reduced during the 12<sup>th</sup> Five-Year Plan period (2011-2015) (Fu et al., 2017).

带格式的: 突出显示

带格式的: 突出显示

带格式的: 突出显示

145 Currently there are strong arguments about the role of regional transport in contributing to haze pollution in China (Guo et al., 2014; Li et al., 2015), especially for severe haze episodes occurring during stagnant meteorological conditions with a shallow boundary layer (Sun et al., 2014; Zheng et al., 2015; Quan et al., 2013). Vertical characterization of air pollutant concentration profiles may be helpful for elucidating factors contributing to the formation and transport of regional haze events (Quan et al., 2013; Tang et al., 2015; Wiegner et al., 2006). Many studies have been conducted to improve our understanding of temporal and spatial concentration dynamics of atmospheric NH<sub>3</sub> and how they relate to underlying factors (e.g. emission intensity, meteorological conditions, etc.) and air quality (Yamamoto et al., 1988; Yamamoto et al., 150 1995; Bari et al., 2003; Vogt et al., 2005; Lee et al., 1999). However, such studies in China have generally focused on the spatial distribution of NH<sub>3</sub> near the ground (Ianniello et al., 2010; Wu et al., 2009; Meng et al., 2011; Xu et al., 2015) and the-vertical characterization of NH<sub>3</sub> concentrations is very limited.

As a trace gas with both point and non-point sources, as well as a tendency to deposit rapidly to surfaces, NH<sub>3</sub> mixing ratios may vary significantly as a function of height. In urban locations, like Beijing, where NH<sub>3</sub> is a key contributor to fine particle formation, local (~~e.g., traffic~~) sources (e.g., traffic) emit at the surface and are then mixed through the boundary layer, while NH<sub>3</sub> transported from agricultural sources outside the city ~~are-is~~ presumably already mixed through the boundary layer. The influence of these behaviors may be reflected in vertical NH<sub>3</sub> concentration gradients measured within the city. For example, dominant local surface traffic emissions might give rise to a profile that peaks near the surface, while ~~NH<sub>3</sub>ammonia~~ transported into the urban area may be uniformly mixed in the vertical or even decline near the surface due to loss by dry deposition. Of course these patterns are expected to be further affected by sinks, including surface deposition as well as fine particle formation of ammonium salts. NH<sub>3</sub> vertical distribution measurements are also useful for advancing satellite retrievals, which offer a great potential for understanding the global distribution of gaseous NH<sub>3</sub> (Shephard and Cady-Pereira, 2015; Sun et al., 2015; Van Damme et al., 2015). 160

165 To our knowledge there are few studies reporting long-term observations of vertical distributions of NH<sub>3</sub> in the lowest few hundred meters of the atmosphere, including measurements at the BAO tower in the USA (Li et al., 2017; Tevlin et al., 2017) and CESAR in The Netherlands (Dammers et al., 2017). Li et al. (2017) analyzed vertical NH<sub>3</sub> concentration profiles at the BAO tower in Colorado, USA, reporting the minimum concentration at the top of the tower, slowly

170 increasing towards a peak concentration at ~10 m before a large reduction in concentration at 1 m. The site was influenced  
by transport of high ammonia-NH<sub>3</sub> concentrations from large animal feeding operations to the northeast. Through higher  
time resolution measurements at the BAO tower, Tevlin et al. (2017) pointed out that the surface can act as an occasional  
NH<sub>3</sub> sink as well as a source. The CESAR study in the Netherlands showed that vertical profile differences were mainly  
due to local and regional transport influences (Dammers et al., 2017)(Li et al., 2017). Because the BAO and CESAR tower  
sites are both located in a-suburban areas with low aerosol mass loadings, observed vertical profiles of aerosol and gas  
175 species (Öztürk et al., 2013; VandenBoer et al., 2013; Riedel et al., 2013) could be substantially different from those in  
megacities in China. Zhou et al. (2017) measured vertical concentration profiles of NH<sub>3</sub> and seven other air pollutants at  
ten heights (8, 15, 47, 80, 120, 160, 200, 240, 280 and 320 m) in urban Beijing, finding NH<sub>3</sub> concentrations peaked at 160  
m. However, ~~only one vertical profile was measured the observation period was too short (two weeks) to investigate  
seasonal variations~~ and may not adequately represent typical conditions. Until now, long-term monitoring of vertical NH<sub>3</sub>  
180 concentration profiles has not been carried out in China.

Here, we report a one-year field campaign on the Beijing 325 m meteorological tower to investigate vertical NH<sub>3</sub>  
concentration profiles and consider how temporal variations may relate to urban emission sources, meteorological factors  
and air transport from more distant sources. Study findings are relevant for our understanding of precursor NH<sub>3</sub>ammonia  
distributions and the role of NH<sub>3</sub>ammonia in the formation of severe aerosol pollution in China, and further provide  
185 benchmarks to assist in meeting air quality goals and policy needs in future.

## 2. Materials and methods

### 2.1 Site Description

The sampling site is located at the State Key Laboratory of Atmospheric Boundary Layer Physics and Atmospheric  
Chemistry (LAPC), Institute of Atmospheric Physics (IAP), Chinese Academy of Sciences (CAS) in urban Beijing (39°58'  
190 N, 116°22'E) (Fig. 1). The site is approximately 0.8 km north of the third Ring Road ~~and~~, 1.3 km south of the fourth Ring  
Road ~~and 0.2 km west of the Beijing-Tibet expressway, which are three major~~ transport arteries encircling Beijing, each

带格式的: 下标



with average traffic volumes of approximately over 200,000+ million vehicles day<sup>-1</sup> in 2016 (Beijing Transport Institute, 2017), representing a typical urban site surrounded mainly by residential areas.

## 2.2 NH<sub>3</sub> measurement

195 From March 16, 2016 to March 16, 2017, weekly atmospheric NH<sub>3</sub> samples were collected at 16 heights on the 325 m meteorological tower using ALPHA passive samplers (adapted low-cost high absorption, Centre for Ecology and Hydrology, Edinburgh, UK) except for a few samples with slightly different duration due to tower the maintenance -of the towerschedules. The samplers operate on the principle of diffusion using an acid-coated filter to capture the NH<sub>3</sub>ammonia. A PTFE (Teflon) membrane is placed directly at the mouth of the sampler, formatting a quiescent minimized-boundary layer in front of the sample membrane. Hence, a stable, turbulent-free diffusion path length is achieved behind the membrane, whilst allowing gaseous NH<sub>3</sub>ammonia to diffuse through for capture and minimizing the sampling of NH<sub>4</sub><sup>+</sup> aerosol (Tang et al., 2014). NH<sub>3</sub> was sampled at 2, 8, 15, 32, 47, 63, 80, 102, 120, 140, 160, 180, 200, 240, 280, and 320 m above ground level. At each height, three ALPHA samplers were deployed under a PVC shelter to protect the samplers from rain and direct sunlight (shown in Fig. 1). Collected NH<sub>3</sub> samplers were extracted with 10 mL high-purity water (18.2 MΩ-cm) and analyzed using a continuous-flow analyzer (Seal AA3, Germany). Three field (travel) blanks were prepared for each batch of samples, analyzed together with those samples, and used to blank correct sample results and determine the minimum-method detection limits (MDL). MDL was calculated using the following equation:  $MDL_{\dots\dots\dots} \geq t \times S_b$   $\times \sqrt{\frac{N_1 + N_2}{N_1 \times N_2}}$ . Ft value given at the 95% confidence level for the appropriate of degrees of freedom. S<sub>b</sub> is the blank standard deviation, N<sub>1</sub> and N<sub>2</sub> is the number of sample measurements (single measurement, N<sub>1</sub>=1), the number of analyzed blanks- using standard deviation of NH<sub>3</sub> concentrations for blank samples multiplied versus the determined one sided t distribution for a 95% confidence level. From the field blanks, the MDL was calculated to be 0.31 μg m<sup>-3</sup> for a one-week ALPHA passive NH<sub>3</sub> sample. All lab measurements were conducted in the Key Laboratory of Plant-Soil Interactions, Chinese Ministry of Education, China Agricultural University. More details of the passive samplers and related laboratory preparation and analysis can be found in Xu et al. (2015).

带格式的：下标  
带格式的：上标

带格式的：下标

带格式的：下标

带格式的：下标

带格式的：下标

带格式的：下标

带格式的：下标

215 2.3 Meteorological data

Meteorological parameters, including wind speed (WS), wind direction (WD), relative humidity (RH), and temperature ( $T$ ), were obtained at all sampling heights except 2 m, and the temperature was not available at 8 m. WS and WD were measured using four-cup anemometers (model O1OC, Met One Instruments), and RH and  $T$  were measured using a  $T$ /RH sensor (model HC2-S3, ROTRONIC).

带格式的: 字体: 倾斜

带格式的: 字体: 倾斜

带格式的: 字体: 倾斜

220 2.4 Data analysis

Repeated-measures analysis of variance (ANOVA) was used to test changes in  $\text{NH}_3$  concentration along vertical profiles. When the ANOVA results were significant, the Tukey's Honest Significant Difference (HSD) test was used to determine the significance of the difference between means with a significance level of  $P < 0.05$ . The coefficient of determination was used to test the linear correlations with a significance level of  $P < 0.05$ . All the statistical analyses were conducted using SPSS Version 23.0 (IBM Corp., Armonk, NY, USA).

带格式的: 字体: 倾斜

带格式的: 字体: 倾斜

Potential source contribution function analysis (PSCF) (Ashbaugh et al., 1985) of atmospheric  $\text{NH}_3$  was performed using Meteoinfo (TrajStat package) (Wang, 2014), where 72 h back trajectories arriving at the monitoring site (IAP tower) at each height were calculated every 3 h for the entire study period. The average  $\text{NH}_3$  concentration for each cluster was computed using the cluster statistics function.  $\text{NH}_3$  pathways could then be associated with the high concentration clusters.

230 The number of trajectory segment endpoints falling in a grid cell ( $i, j$ ) is  $n_{ij}$ . The number of trajectory endpoints associated with the data with the concentration of  $\text{NH}_3$  concentrations higher than an arbitrarily set criterion for each height during the four seasons (75<sup>th</sup> percentile for  $\text{NH}_3$  was set here) is  $m_{ij}$  (Table S1). The PSCF value for the  $ij^{\text{th}}$  cell is then calculated as  $m_{ij}/n_{ij}$ . A weighting function  $W_{ij}$  was applied to reduce the uncertainties of small values of  $n_{ij}$  (Polissar et al., 1999). Weighted PSCF values (WPSCF) were calculated by multiplying a particular  $W_{ij}$  ( $\leq 1.00$ ) if the total number of the endpoints for one grid cell was lower than three times the average of the endpoints per each cell. Higher WPSCF values indicate higher potential contributions of  $\text{NH}_3$  to the receptor site (IAP tower).

带格式的: 突出显示

$$w_{ij} = \begin{cases} 1.00 & 80 < n_{ij} \\ 0.70 & 20 < n_{ij} \leq 80 \\ 0.42 & 10 < n_{ij} \leq 20 \\ 0.05 & n_{ij} \leq 10 \end{cases}$$

### 3. Results

#### 3.1 Vertical profiles of NH<sub>3</sub> concentrations

240 The time series of weekly averages of NH<sub>3</sub> concentrations during March 16, 2016 - March 16, 2017 are shown in Fig. 2. The weekly NH<sub>3</sub> concentration across all heights averaged 13.3±4.8 μg m<sup>-3</sup> during the year-long study period. Individual weekly concentrations ranged from 4.4 μg m<sup>-3</sup> at 2 m to 25.3 μg m<sup>-3</sup> at 32 m. **Nearly all (99.6%)** of the weekly NH<sub>3</sub> concentrations along the profile exceeded 5 μg m<sup>-3</sup>. Summer concentrations were generally the highest. Maximum NH<sub>3</sub> concentrations mostly occurred between 32 m and 63 m, decreasing both towards the surface and the top of the tower. Minimum concentrations mostly occurred at 2 m and 320 m (Fig. S1). Significant differences of annual average NH<sub>3</sub> concentrations across the vertical profile were only found between the “maximum concentration” height and the top two heights, i.e. 280 m and 320 m (Fig. 3i). Even at 320 m, the annual average NH<sub>3</sub> concentration was still relatively high at 11.3 μg m<sup>-3</sup> (Fig. 3i). During the whole **Beijing**-observation period, the daily average boundary layer height was generally above 320 m, indicating a good portion of the sampling occurred within a well-mixed boundary layer (Fig. S2).

250 Seasonal vertical concentration profiles exhibited fairly similar shapes ~~that were fairly similar to that of~~ the annual average profile, ~~but yet~~ with some important differences in absolute concentration values and the magnitude of vertical gradients within the profiles (Fig. 3). The average NH<sub>3</sub> concentration across the profile from high to low was observed in summer (18.2 μg m<sup>-3</sup>), spring (13.4 μg m<sup>-3</sup>), autumn (12.1 μg m<sup>-3</sup>), and winter (8.3 μg m<sup>-3</sup>). Proportional declines of NH<sub>3</sub> concentration from the peak to higher and lower elevations differed between seasons, being the greatest in autumn (28.31% decrease from 63 m to 320 m), and winter (27.23.8%) followed by **summer** (19.720.5%) and spring (15.48%) (Fig. S3).

带格式的: 突出显示

带格式的: 字体颜色: 自动设置

带格式的: 突出显示

### 3.2 Meteorological variability

Vertical NH<sub>3</sub> concentration profiles varied substantially during the sampling period, along with vertical changes in meteorological parameters. Bivariate polar plots (Fig. 4) show that high NH<sub>3</sub> concentrations below 47 m were mostly observed during periods with low wind speeds (< 4 m s<sup>-1</sup>). As heights and associated wind speeds increased, the relationship between NH<sub>3</sub> concentrations and wind speed weakened. For example, at 280 m, the highest concentration was observed when the wind speed was also high (up to an average of ~15 m s<sup>-1</sup>).

Wind directions play an important role in air pollution transport. Transport from the northwest was typically associated with low NH<sub>3</sub> concentrations at all heights, consistent with the absence of large emissions sources in the mountains NW of Beijing. It is noteworthy that high NH<sub>3</sub> concentrations at near-surface heights (8 m and 15 m) always coincide with winds from the south, including southeast and southwest directions. High NH<sub>3</sub> concentrations appear to be associated with winds from the northeast from 32 m until 80 m. Above 80 m, winds from the south contribute more to high NH<sub>3</sub> concentrations. Major regions of agricultural NH<sub>3</sub> emissions are located south and east of Beijing.

To further investigate observed variability, we show the probability density function of NH<sub>3</sub> concentrations in relation to the relative humidity (RH) and temperature ( $T$ ) (Fig. 5). Clear positive relationships between  $T$  and NH<sub>3</sub> concentrations were found at all heights from low RH to high RH. When  $T$  was low ( $T < 12^\circ\text{C}$ ), the NH<sub>3</sub> concentration fell mostly below 10  $\mu\text{g m}^{-3}$  under any RH condition. The occurrence of high NH<sub>3</sub> concentrations increased with higher  $T > 12^\circ\text{C}$ , which is not surprising, given that agricultural NH<sub>3</sub> emissions increase with  $T$  while higher  $T$  and lower RH also shift the equilibrium of the  $\text{NH}_3(\text{g}) + \text{HNO}_3(\text{g}) \leftrightarrow \text{NH}_4\text{NO}_3(\text{p})$  system toward the gas phase. Statistically, a strong positive relationship was found between NH<sub>3</sub> and  $T$  at all heights from the surface to the top of the tower ( $R^2 \sim 0.6$ ) (Fig. S4); both slope and correlation coefficients were similar across all heights. Although, a positive correlation between NH<sub>3</sub> and RH and a negative correlation between NH<sub>3</sub> and wind speed (WS) were found, the correlation coefficients were quite low.

### 3.3 Potential source analysis

Analysis of the relationship between local wind direction and NH<sub>3</sub> concentrations does not fully clarify the potential source regions contributing to observed NH<sub>3</sub> ammonia at the sampling site (Fig. S6). Some seasonal variations were observed

带格式的: 字体: 倾斜

带格式的: 字体: 倾斜

带格式的: 字体: 倾斜

带格式的: 字体: 倾斜

带格式的: 字体: 倾斜

带格式的: 字体: 倾斜

带格式的: 突出显示

带格式的: 突出显示

带格式的: 突出显示

带格式的: 字体: 倾斜

~~related to season, such as i.e. the frequency of high NH<sub>3</sub> concentration was higher~~ greater with southerly winds than ~~northwesterly winds~~ increased as wind sectors changed from northwest to south in the spring, ~~higher~~ increased frequency of high NH<sub>3</sub> concentrations were associated with southerly and easterly winds in the summer and autumn, and NH<sub>3</sub> concentrations still exceeded 5 μg m<sup>-3</sup> during winter with relatively frequent winds from ~~north and the~~ northwest.

带格式的: 下标

285 To examine the relationship between air transport and ~~NH<sub>3</sub> ammonia~~ concentrations more rigorously, weighted PSCF (WPSCF) during the four seasons were calculated for several measurement heights (2, 63, 180, 320 m) (Fig. 6). In summer, from the surface to the tower top, a strong influence is seen from source areas to the south of Beijing, coinciding with regions (e.g. Tianjin, Henan, Hebei and Shandong provinces) characterized by elevated anthropogenic emissions of NH<sub>3</sub> (Fig. 1), largely from agricultural activities (Zhang et al., 2009; Gu et al., 2012). During summer, regions to the north and 290 west of the monitoring site had low WPSCF values. High WPSCF values to the south and southeast were common during spring. High WPSCF values were mainly located northwest and southeast of Beijing in autumn, while ~~there~~ their WPSCF values were typically lower in winter than during other seasons.

It is important to remember that aerosol-gas partitioning can also strongly influence measured NH<sub>3</sub> concentrations. To investigate seasonal phase changes between NH<sub>3</sub> and NH<sub>4</sub><sup>+</sup>, we define the ~~NH<sub>3</sub> ammonia~~ gas fraction ( $F_{\text{NH}_3}$  = the gaseous 295 NH<sub>3</sub> concentration divided by the sum of the gaseous NH<sub>3</sub> and fine particulate NH<sub>4</sub><sup>+</sup> concentrations), where the concentrations are expressed in molar units. Monthly average partitioning for these reduced inorganic nitrogen forms from a nearby urban monitoring site, 10 km away from the IAP tower, is plotted in Fig. S8. The NH<sub>3</sub> gas fraction ( $F_{\text{NH}_3}$ ) was found to be the highest in summer (0.83 in August) and the lowest in winter (0.36 in February). As expected, gas phase NH<sub>3</sub> is favored in the warmer months, while particle phase NH<sub>4</sub><sup>+</sup> is favored for the cooler months, with a gradual transition. 300 Weekly NH<sub>4</sub><sup>+</sup> concentrations at the tower were estimated using weekly NH<sub>3</sub> concentrations divided by monthly  $F_{\text{NH}_3}$ , then, WPSCF analysis of the sum of NH<sub>3</sub>+NH<sub>4</sub><sup>+</sup> was performed (see results in Fig. S9). Results of this total WPSCF (NH<sub>3</sub>+NH<sub>4</sub><sup>+</sup>) analysis yielded similar patterns to the NH<sub>3</sub> WPSCF analysis for all heights and seasons, indicating the importance of the identified source regions for both the gaseous and particulate atmospheric forms of emitted NH<sub>3</sub>.

## 4. Discussion

### 4.1 Vertical NH<sub>3</sub> concentration profiles

The North China Plain is a well-known “hotspot” for NH<sub>3</sub> emissions due to the rapid development of industrialization, urbanization and intensive agriculture (Kang et al., 2016; Zhang et al., 2010). In our study, high atmospheric NH<sub>3</sub> concentrations (13.3±4.8 μg m<sup>-3</sup>) were found up to 320 m above ground level in urban Beijing (March 16<sup>th</sup>, 2016 - March 16<sup>th</sup>, 2017), much higher than the average annual NH<sub>3</sub> concentration (3.3±1.4 μg m<sup>-3</sup>) observed across a vertical profile at the 300 m USA rural BAO tower (Li et al., 2017). Some studies of NH<sub>3</sub> vertical distribution found that the NH<sub>3</sub> concentration significantly decreased with height. For example, Tevlin et al. (2017) reported an overall increase in summertime NH<sub>3</sub> mixing ratios toward the surface of 6.7 ppb or 5.1 μg m<sup>-3</sup> (89%) during the day and 3.9 ppb or 3.0 μg m<sup>-3</sup> (141%) at night. In the BAO tower study (Li et al., 2017), which also measured concentrations using passive (Radiello) samplers deployed for one to two week sample periods, the concentration profiles showed a similar overall vertical distribution. The minimum NH<sub>3</sub> concentration was at the top, slowly increasing towards a peak concentration at ~10 m before a sharp reduction near the surface. By contrast, our results showed much smaller decreases in NH<sub>3</sub> concentrations in upper air in urban Beijing (Table 1), with only a 1.18 μg m<sup>-3</sup> (9.5%) average decrease from the surface to the top (Fig. 3i). The flatter shape of the Beijing vertical profile may reflect a combination of strong local (e.g. vehicle) and regional (e.g. industrial and agricultural emissions) sources (Fig. 2 and Fig.6) in our study, the fact that deep mixing layers regularly enveloped the full height of the tower within the surface boundary layer so that all sources influencing the tower measurements were vertically well mixed (Fig. S2), and/or the averaging of more distinct profiles over the week-long sample periods. In contrast to the “rural” boundary layer above the fields surrounding the BAO tower, the mixing in the Beijing urban area could be greatly enhanced by larger surface roughness (e.g. average urban building height being ~50 m) and surface heating (Baklanov and Kuchin, 2004). Higher time resolution vertical profile measurements are needed in the future to untangle the influence of these potential factors.

Distinct seasonal variations in NH<sub>3</sub> concentrations were found (Fig. 2), statistically most strongly associated with temperature rather than relative humidity or wind speed (Fig. S4). High temperatures enhance NH<sub>3</sub> emissions from soil,

带格式的: 突出显示

带格式的: 突出显示

带格式的: 突出显示

applied fertilizers, ~~and~~ animal waste, ~~can enhance~~ vertical mixing, and increase volatilization of NH<sub>3</sub> from NH<sub>4</sub>NO<sub>3</sub> particulate matter (Bari et al., 2003; Ianniello et al., 2010; Li et al., 2014; Lin et al., 2006; Meng et al., 2011; Plessow et al., 2005; Walker et al., 2004; Zbieranowski and Aherne, 2012). While high (low) mixed-layer heights in spring and summer (autumn and winter) could dilute (concentrate) NH<sub>3</sub> in the surface boundary layer (Fig. S3), average NH<sub>3</sub> concentrations across the profile were actually high in summer/spring and low in winter/autumn, consistent with the strong temperature-driven seasonal variation of NH<sub>3</sub> concentration and the greater NH<sub>4</sub>NO<sub>3</sub> particle formation during cold periods in autumn and winter. ~~Conducting~~~~Having~~ simultaneous measurements of fine particle composition, ~~with at different~~ heights, in future studies would be valuable for more closely evaluating the influence of changes in phase-partitioning.

Li et al. (2017) found ~~(Fig. 3j)~~ a vertical difference of approximately 75% from the concentration peak near the surface to the top of the BAO tower in winter (Fig. 3j), and attributed this strong vertical gradient to the occurrence of low level temperature inversions which trapped emissions closer to the surface in winter. During our study in Beijing, the vertical gradient was only 28% in winter (maximum concentration found at 32 m), consistent with a deeper average boundary layer. Inversions, however, did limit vertical mixing of NH<sub>3</sub> during some periods in Beijing. Examination of thermal inversion layer probability at 6 a.m. and 3 p.m. (Fig. S7b and 7c) revealed that T inversions (0.22±0.26 °C) frequently occurred between 102 m and 160 m. Consequently, persistent higher NH<sub>3</sub> concentrations begin at a lower altitude (Fig. S7a) as also observed by Tevlin et al. (2017). Because the time resolution of our Beijing study was one sample per week, we could not catch the changes between the daytime and nighttime NH<sub>3</sub> vertical mixing. Compared to NH<sub>3</sub> monitoring in real time (Tevlin et al., 2017), weekly sampling smooths diurnal vertical distributions and makes it harder to identify the influence of local, surface sources or sinks.

Surfaces can act either as sources or sinks of NH<sub>3</sub>, depending on surface NH<sub>3</sub> content, ambient NH<sub>3</sub> concentrations, ~~and~~ local meteorology and surface type (Tevlin et al., 2017; Zhang et al., 2010). The maximum NH<sub>3</sub> concentration occurrence at 2 m in Beijing and the concentration decrease with increased height may reflect an important surface source of NH<sub>3</sub>, although our limited time resolution makes such conclusions tentative. The influence of evaporation of dew/precipitation may also be important. Some studies found that dew is both a significant night-time reservoir/sink and strong morning source of NH<sub>3</sub> (Wentworth et al., 2016; Teng et al., 2017).

带格式的: 字体: 倾斜

带格式的: 突出显示

带格式的: 突出显示

#### 4.2. Potential source analysis

Areas south of Beijing with high WPSCF values appear to be important NH<sub>3</sub> source regions (Fig. 6), suggesting regional transport from high agricultural NH<sub>3</sub> emission areas (e.g. Hebei, Henan, Shandong provinces etc.) contributed significantly to atmospheric NH<sub>3</sub> in the Beijing urban region. Consistently higher NH<sub>3</sub> concentrations were observed during periods with winds from the SE, S and SW at all heights, especially in summer (Fig. S6). Although NH<sub>3</sub> has a limited atmospheric lifetime with respect to dry deposition, concentrations in these agricultural NH<sub>3</sub> source regions can be extremely high (Shen et al., 2011) while significant ~~NH<sub>3</sub> ammonia~~ can be tied up in longer-lived ammonium nitrate particles that partially dissociate to release NH<sub>3</sub> back to the gas phase in response to NH<sub>3</sub> loss by dry deposition (Ianniello et al., 2011; Kang et al., 2016; Xu et al., 2017). The WPSCF (Fig. 6) and NH<sub>3</sub> emissions distribution (Fig. 1 left) both suggest the importance not only of regional transport from nearby areas, but also the potential for local emissions to play an important role in sustaining the high NH<sub>3</sub> level in Beijing, e.g. vehicular traffic (Chang et al., 2018; Pan et al., 2018a). As discussed above, stagnant meteorological conditions with low WS and ~~T inversions allow local emissions, such as those from urban traffic,~~ to accumulate. Additionally, the topography of the mountains to the west and north of Beijing effectively traps polluted air over Beijing during southerly airflow, an effect reported in many Beijing particulate matter studies (Xia et al., 2016; Wu et al., 2009; Zhao et al., 2009).

Generally, NH<sub>3</sub> source regions identified in WPSCF analysis (Fig. 6) suggested that regional transport from the south exerts an important influence on Beijing NH<sub>3</sub> concentrations throughout the year. The area south of Beijing (e.g. Hebei, Henan and Shandong provinces) is a hotspot of NH<sub>3</sub> emission (Zhang et al., 2018) and half of NH<sub>3</sub> emissions have been estimated to deposit as NH<sub>3</sub> at urban sites in North China Plain (Pan et al., 2018b). In addition, seasonal patterns of NH<sub>3</sub> potential sources (Fig. 6) matched well with the seasonal surface NH<sub>3</sub> concentrations in China (Zhang et al., 2018). In detail, NH<sub>3</sub> concentrations were typically highest in summer and south winds produced higher NH<sub>3</sub> concentrations than other ~~summer~~-wind directions (Fig. S6). Spring and summer had a similar wind direction distribution (Fig. S6) and wind speeds (Fig. S5), but corresponding NH<sub>3</sub> concentrations were lower in spring. This may reflect decreased emissions in regions to the south during cooler spring temperatures and increased partitioning of NH<sub>3</sub> into fine particles during this

带格式的: 字体: 倾斜



cooler season. As shown above aerosol-gas partitioning strongly influences  $\text{NH}_3$  concentrations; high  $F_{\text{NH}_3}$  during warm periods, especially summer, favored greater  $\text{NH}_3$  gas concentrations due to the thermodynamic tendency for  $\text{NH}_4\text{NO}_3$  to dissociate to  $\text{NH}_3$  and  $\text{HNO}_3$  at high temperature. Although  $F_{\text{NH}_3}$  was low in winter, indicating  $\text{NH}_4^+$  is the dominant  $\text{NH}_x$  form in this cold season, winter  $\text{NH}_3$  concentrations across all heights still averaged  $8.3 \pm 2.6 \mu\text{g m}^{-3}$ , with a similar wind direction distribution as other seasons, except at high altitudes (i.e. 240 m and 320 m, Fig. S6).

## 5. Conclusions and implications

Our study is the first to continually monitor the vertical concentration profile of  $\text{NH}_3$  in urban Beijing. Weekly concentrations were measured for one year at 16 heights on the ~~325-m~~ Beijing 325 m meteorological tower. The  $\text{NH}_3$  concentration averaged  $13.3 \pm 4.8 \mu\text{g m}^{-3}$ . The Highest-highest  $\text{NH}_3$  concentrations were always observed at 32-63 m height, decreasing toward the surface and toward higher altitudes.

$\text{NH}_3$  concentrations at all heights increased during warmer periods, consistent with increased  $\text{NH}_3$  emissions under warm conditions and the tendency for semivolatile ammonium nitrate to release  $\text{NH}_3$  to the gas phase. Analysis of the relationship between  $\text{NH}_3$  concentrations and local wind direction showed a tendency for higher concentrations during transport from regions to the south of Beijing, consistent with findings from WPSCF analysis that showed that important source areas were mainly located to the south of Beijing, consistent with large agricultural regions and high  $\text{NH}_3$  emissions in the North China Plain. Local  $\text{NH}_3$  sources, such as urban traffic emissions, may also help account for the elevated  $\text{NH}_3$  concentrations ( $> 5 \mu\text{g m}^{-3}$ ) observed even in periods when transport came mostly from low  $\text{NH}_3$  mountainous regions to Beijing's north/northwest.

High  $\text{NH}_3$  concentrations in urban Beijing, from the surface up to 320 m, the important role that  $\text{NH}_3$  plays in  $\text{PM}_{2.5}$  and haze formation, and the importance of regional transport of  $\text{NH}_3$  emissions from agricultural regions in neighboring provinces, suggest that future air quality improvement efforts should consider  $\text{NH}_3$  emission reductions and that the pollution controls should be jointly practiced at regional scales (e.g. the whole North China Plain) rather than only controlling local Beijing sources.

400 *Acknowledgements.* This work was supported by the State Key Research & Development Programme (2016YFC0207906,  
2017YFC0210100, DQGG0208), the National Natural Science Foundation of China (41425007, [91744207](#)), and the  
National Postdoctoral Program for Innovative Talents (BX201600157).

## References

Ashbaugh, L. L., Malm, W. C., and Sadeh, W. Z.: A residence time probability analysis of sulfur concentrations at Grand  
405 Canyon National Park, *Atmos. Environ.* (1967), 19, 1263-1270, [https://doi.org/10.1016/0004-6981\(85\)90256-2](https://doi.org/10.1016/0004-6981(85)90256-2), 1985.

[Baklanov, A. and Kuchin, A.: The mixing height in urban areas: comparative study for Copenhagen, \*Atmos. Chem. Phys. Discuss.\*, 4, 2839-2866, <https://doi.org/10.5194/acpd-4-2839-2004>, 2004.](#)

Bari, A., Ferraro, V., Wilson, L. R., Luttinger, D., and Husain, L.: Measurements of gaseous HONO, HNO<sub>3</sub>, SO<sub>2</sub>, HCl,  
410 NH<sub>3</sub>, particulate sulfate and PM<sub>2.5</sub> in New York, NY, *Atmos. Environ.*, 37, 2825-2835,  
[https://doi.org/10.1016/S1352-2310\(03\)00199-7](https://doi.org/10.1016/S1352-2310(03)00199-7), 2003.

[Beijing Transport Institute: Annual report of Beijing traffic development in 2017, <http://www.bjtrc.org.cn/JGJS.aspx?id=5.2&Menu=GZCG>, 2017.](#)

Chang, Y., Liu, X., Deng, C., Dore, A. J., and Zhuang, G.: Source apportionment of atmospheric ammonia before, during,  
415 and after the 2014 APEC summit in Beijing using stable nitrogen isotope signatures, *Atmos. Chem. Phys.*, 16,  
11635-11647, <https://doi.org/10.5194/acp-16-11635-2016>, 2016.

Dammers, E., Schaap, M., Haaima, M., Palm, M., Kruit, R. W., Volten, H., Hensen, A., Swart, D., and Erisman, J.:  
Measuring atmospheric ammonia with remote sensing campaign: Part 1—Characterisation of vertical ammonia  
concentration profile in the centre of The Netherlands, *Atmos. Environ.*, 169, 97-112,  
<https://doi.org/10.1016/j.atmosenv.2017.08.067>, 2017.

420 EMEP Webdab emission data hosted by the Centre on Emission Inventories and Projections (CEIP): <http://www.ceip.at>,  
access: 20 August, 2018<sup>09</sup>.

Erisman, J. W., Vermetten, A. W., Asman, W. A., Waijers-Ijpelaar, A., and Slanina, J.: Vertical distribution of gases and

带格式的: 英语(美国)

aerosols: the behaviour of ammonia and related components in the lower atmosphere, *Atmos. Environ.* (1967), 22, 1153-1160, [https://doi.org/10.1016/0004-6981\(88\)90345-9](https://doi.org/10.1016/0004-6981(88)90345-9), 1988.

425 Erisman, J. W., Sutton, M. A., Galloway, J., Klimont, Z., and Winiwarter, W.: How a century of ammonia synthesis changed the world, *Nat. Geosci.*, 1, 636-639, <https://doi.org/10.1038/ngeo325>, 2008.

Fowler, D., Pilegaard, K., Sutton, M., Ambus, P., Raivonen, M., Duyzer, J., Simpson, D., Fagerli, H., Fuzzi, S., and Schjørring, J. K.: Atmospheric composition change: ecosystems-atmosphere interactions, *Atmos. Environ.*, 43, 5193-5267, <https://doi.org/10.1016/j.atmosenv.2009.07.068>, 2009.

430 Fu, X., Wang, S., Xing, J., Zhang, X., Wang, T., and Hao, J.: Increasing Ammonia Concentrations Reduce the Effectiveness of Particle Pollution Control Achieved via SO<sub>2</sub> and NO<sub>x</sub> Emissions Reduction in East China, *Environ. Sci. Technol. Letters*, 4, 221-227, <https://doi.org/10.1021/acs.estlett.7b00143>, 2017.

Galloway, J. N., Aber, J. D., Erisman, J. W., Seitzinger, S. P., Howarth, R. W., Cowling, E. B., and Cosby, B. J.: The nitrogen cascade, *AIBS Bulletin*, 53, 341-356, [https://doi.org/10.1641/0006-3568\(2003\)053\[0341:TNC\]2.0.CO;2](https://doi.org/10.1641/0006-3568(2003)053[0341:TNC]2.0.CO;2),  
435 2003.

Gu, B., Ge, Y., Ren, Y., Xu, B., Luo, W., Jiang, H., Gu, B., and Chang, J.: Atmospheric reactive nitrogen in China: Sources, recent trends, and damage costs, *Environ. Sci. Technol.*, 46, 9420-9427, <https://doi.org/10.1021/es301446g>,  
2012.

Gu, B., Sutton, M. A., Chang, S. X., Ge, Y., and Chang, J.: Agricultural ammonia emissions contribute to China's urban air  
440 pollution, *Front. Ecol. Environ.*, 12, 265-266, <https://doi.org/10.1890/14.WB.007>, 2014.

Guo, S., Hu, M., Zamora, M. L., Peng, J., Shang, D., Zheng, J., Du, Z., Wu, Z., Shao, M., and Zeng, L.: Elucidating severe urban haze formation in China, [Proc. Natl. Acad. Sci. USA, Proceedings of the National Academy of Sciences of the United States of America](https://doi.org/10.1073/pnas.1419604111), 111, 17373-17378, <https://doi.org/10.1073/pnas.1419604111>, 2014.

Huang, R., Zhang, Y., Bozzetti, C., Ho, K., Cao, J., Han, Y., Daellenbach, K. R., Slowik, J. G., Platt, S. M., and Canonaco,  
445 F.: High secondary aerosol contribution to particulate pollution during haze events in China, *Nature*, 514, 218-222, <https://doi.org/10.1038/nature13774>, 2014.

Ianniello, A., Spataro, F., Esposito, G., Allegrini, I., Rantica, E., Ancora, M., Hu, M., and Zhu, T.: Occurrence of gas phase

ammonia in the area of Beijing (China), *Atmos. Chem. Phys.*, 10, 9487-9503, <https://doi.org/10.5194/acp-10-9487-2010>, 2010.

450 Ianniello, A., Spataro, F., Esposito, G., Allegrini, I., Hu, M., and Zhu, T.: Chemical characteristics of inorganic ammonium salts in PM<sub>2.5</sub> in the atmosphere of Beijing (China), *Atmos. Chem. Phys.*, 11, 10803-10822, <https://doi.org/10.5194/acp-11-10803-2011>, 2011.

Kang, Y., Liu, M., Song, Y., Huang, X., Yao, H., Cai, X., Zhang, H., Kang, L., Liu, X., and Yan, X.: High-resolution ammonia emissions inventories in China from 1980 to 2012, *Atmos. Chem. Phys.*, 16, 2043-2058, <https://doi.org/10.5194/acp-16-2043-2016>, 2016.

455 Klimont, Z.: Current and Future Emissions of Ammonia in China, 10<sup>th</sup> annual emission inventory conference: one atmosphere, One inventory, many challenges, 1-3, May, 2001

LeBel, P. J., Hoell, J. M., Levine, J. S., and Vay, S. A.: Aircraft measurements of ammonia and nitric acid in the lower troposphere, *Geophys. Res. Lett.*, 12, 401-404, <https://doi.org/10.1029/GL012i006p00401>, 1985.

460 Lee, D., Dollard, G., Derwent, R., and Pepler, S.: Observations on gaseous and aerosols components of the atmosphere and their relationships, *Water, Air & Soil Pollut.*, 113, 175-202, 1999.

Li, P., Yan, R., Yu, S., Wang, S., Liu, W., and Bao, H.: Reinstate regional transport of PM<sub>2.5</sub> as a major cause of severe haze in Beijing, *Proceedings of the National Academy of Sciences of the United States of America*, 112, E2739-E2740, <https://doi.org/10.1073/pnas.1502596112>, 2015.

465 Li, Y., Schwandner, F. M., Sewell, H. J., Zivkovich, A., Tigges, M., Raja, S., Holcomb, S., Molenaar, J. V., Sherman, L., and Archuleta, C.: Observations of ammonia, nitric acid, and fine particles in a rural gas production region, *Atmos. Environ.*, 83, 80-89, <https://doi.org/10.1016/j.atmosenv.2013.10.007>, 2014.

470 Li, Y., Thompson, T. M., Damme, M. V., Chen, X., Benedict, K. B., Shao, Y., Day, D., Boris, A., Sullivan, A. P., and Ham, J.: Temporal and spatial variability of ammonia in urban and agricultural regions of northern Colorado, United States, *Atmos. Chem. Phys.*, 17, 6197-6213, <https://doi.org/10.5194/acp-17-6197-2017>, 2017.

Lin, Y., Cheng, M., Ting, W., and Yeh, C.: Characteristics of gaseous HNO<sub>2</sub>, HNO<sub>3</sub>, NH<sub>3</sub> and particulate ammonium nitrate in an urban city of Central Taiwan, *Atmos. Environ.*, 40, 4725-4733, 20

带格式的: 上标

<https://doi.org/10.1016/j.atmosenv.2006.04.037>, 2006.

[Liu, X., Zhang, Y., Han, W., Tang, A., Shen, J., Cui, Z., Vitousek, P., Erisman, J. W., Goulding K., Christie, P., Fangmeier, A., Zhang, F.: Enhanced nitrogen deposition over China. Nature, 494, 459-462, <https://doi:10.1038/nature11917>, 2013](#)

Meng, Z., Lin, W., Jiang, X., Yan, P., Wang, Y., Zhang, Y., Jia, X., and Yu, X.: Characteristics of atmospheric ammonia over Beijing, China, *Atmos. Chem. Phys.*, 11, 6139-6151, <https://doi.org/10.5194/acp-11-6139-2011>, 2011.

Öztürk, F., Bahreini, R., Wagner, N., Dubé, W., Young, C., Brown, S., Brock, C., Ulbrich, I., Jimenez, J., and Cooper, O.: Vertically resolved chemical characteristics and sources of submicron aerosols measured on a Tall Tower in a suburban area near Denver, Colorado in winter, *J. Geophys. Res. [Atmos.]*, 118, 13591-13605, <https://doi.org/10.1002/2013JD019923>, 2013.

Pan, Y., Tian, S., Liu, D., Fang, Y., Zhu, X., Gao, M., Gao, J., Michalski, G., and Wang, Y.: Isotopic evidence for enhanced fossil fuel sources of aerosol ammonium in the urban atmosphere, *Environ. Pollut.*, 238, 942-947, <https://doi.org/10.1016/j.envpol.2018.03.038>, 2018a.

Pan, Y., Tian, S., Zhao, Y., Zhang, L., Zhu, X., Gao, J., Huang, W., Zhou, Y., Song, Y., and Zhang, Q.: Identifying ammonia hotspots in China using a national observation network, *Environ. Sci. Technol.*, 52, 3926-3934, <https://doi.org/10.1021/acs.est.7b05235>, 2018b.

Plessow, K., Spindler, G., Zimmermann, F., and Matschullat, J.: Seasonal variations and interactions of N-containing gases and particles over a coniferous forest, Saxony, Germany, *Atmos. Environ.*, 39, 6995-7007, <https://doi.org/10.1016/j.atmosenv.2005.07.046>, 2005.

Polissar, A., Hopke, P., Paatero, P., Kaufmann, Y., Hall, D., Bodhaine, B., Dutton, E., and Harris, J.: The aerosol at Barrow, Alaska: long-term trends and source locations, *Atmos. Environ.*, 33, 2441-2458, [https://doi.org/10.1016/S1352-2310\(98\)00423-3](https://doi.org/10.1016/S1352-2310(98)00423-3), 1999.

Quan, J., Gao, Y., Zhang, Q., Tie, X., Cao, J., Han, S., Meng, J., Chen, P., and Zhao, D.: Evolution of planetary boundary layer under different weather conditions, and its impact on aerosol concentrations, *Particuology*, 11, 34-40, <https://doi.org/10.1016/j.partic.2012.04.005>, 2013.

带格式的: 字体: 非倾斜, 无下划线

Reis, S., Pinder, R., Zhang, M., Lijie, G., and Sutton, M.: Reactive nitrogen in atmospheric emission inventories, *Atmos. Chem. Phys.* , 9, 7657-7677, <https://doi.org/10.5194/acp-9-7657-2009>, 2009.

500 Riedel, T. P., Wagner, N. L., Dubé, W. P., Middlebrook, A. M., Young, C. J., Öztürk, F., Bahreini, R., VandenBoer, T. C., Wolfe, D. E., and Williams, E. J.: Chlorine activation within urban or power plant plumes: Vertically resolved ClNO<sub>2</sub> and Cl<sub>2</sub> measurements from a tall tower in a polluted continental setting, *J. Geophys. Res. [Atmos.]*, 118, 8702-8715, <https://doi.org/10.1002/jgrd.50637>, 2013.

Shen, J., Liu, X., Zhang, Y., Fangmeier, A., Goulding, K., and Zhang, F.: Atmospheric ammonia and particulate ammonium from agricultural sources in the North China Plain, *Atmos. Environ.*—, 45, 5033-5041, <https://doi.org/10.1016/j.atmosenv.2011.02.031>, 2011.

Shephard, M., and Cady-Pereira, K.: Cross-track Infrared Sounder (CrIS) satellite observations of tropospheric ammonia, *Atmos. Meas. Tech.*, 8, 1323-1336, <https://doi.org/10.5194/amt-8-1323-2015>, 2015.

Sun, K., Tao, L., Miller, D. J., Zondlo, M. A., Shonkwiler, K. B., Nash, C., and Ham, J. M.: Open-path eddy covariance measurements of ammonia fluxes from a beef cattle feedlot, *Agric. For. Meteorol.* , 213, 193-202, <https://doi.org/10.1016/j.agrformet.2015.06.007>, 2015.

Sun, K., Tao, L., Miller, D. J., Pan, D., Golston, L. M., Zondlo, M. A., Griffin, R. J., Wallace, H. W., Leong, Y. J., and Yang, M. M.: Vehicle emissions as an important urban ammonia source in the United States and China, *Environ. Sci. Technol.*—, 51, 2472-2481, <https://doi.org/10.1021/acs.est.6b02805>, 2017.

515 Sun, Y., Jiang, Q., Wang, Z., Fu, P., Li, J., Yang, T., and Yin, Y.: Investigation of the sources and evolution processes of severe haze pollution in Beijing in January 2013, *J. Geophys. Res. [Atmos.]*, 119, 4380-4398, <https://doi.org/10.1002/2014JD021641>, 2014.

Sun, Y., Du, W., Fu, P., Wang, Q., Li, J., Ge, X., Zhang, Q., Zhu, C., Ren, L., and Xu, W.: Primary and secondary aerosols in Beijing in winter: sources, variations and processes, *Atmos. Chem. Phys.*—, 16, 8309-8329, <https://doi.org/10.5194/acp-16-8309-2016>, 2016.

Sutton, M. A., Erismann, J. W., Dentener, F., and Möller, D.: Ammonia in the environment: from ancient times to the present, *Environ. Pollut.* , 156, 583-604, <https://doi.org/10.1016/j.envpol.2008.03.013>, 2008.

525 Tang, G., Zhu, X., Hu, B., Xin, J., Wang, L., Münkkel, C., Mao, G., and Wang, Y.: Impact of emission controls on air quality in Beijing during APEC 2014: lidar ceilometer observations, *Atmos. Chem. Phys.*, 15, 12667-12680, <https://doi.org/10.5194/acp-15-12667-2015>, 2015.

[Tang, Y. S., Cape, J. N., and Sutton, M. A.: Development and types of passive samplers for monitoring atmospheric NO<sub>2</sub> and NH<sub>3</sub> concentrations, \*Scientific World Journal\*, 1, 513-529, <https://doi.org/10.1100/tsw.2001.82>, 2014.](#)

带格式的: 下标

带格式的: 下标

530 Teng, X., Hu, Q., Zhang, L., Qi, J., Shi, J., Xie, H., Gao, H., and Yao, X.: Identification of major sources of atmospheric NH<sub>3</sub> in an urban environment in northern China during wintertime, *Environ. Sci. Technol.*, 51, 6839-6848, <https://doi.org/10.1021/acs.est.7b00328>, 2017.

Tevlin, A., Li, Y., Collett, J., McDuffie, E., Fischer, E., and Murphy, J.: Tall tower vertical profiles and diurnal trends of ammonia in the Colorado Front Range, *J. Geophys. Res. [Atmos.]*, 122, 12468-12487, <https://doi.org/10.1002/2017JD026534>, 2017.

535 [USEPA National Emission Inventory Tier Summaries: <https://www.epa.gov/ttn/chief/eiinformation.html>, access: 14 August 2009](#); [USEPA: Air Pollutant Emissions Trends Data, <https://www.epa.gov/air-emissions-inventories/air-pollutant-emissions-trends-data>, access: 15 October 2018.](#)

Van Damme, M., Clarisse, L., Dammers, E., Liu, X., Nowak, J., Clerbaux, C., Flechard, C., Galy-Lacaux, C., Xu, W., and Neuman, J.: Towards validation of ammonia (NH<sub>3</sub>) measurements from the IASI satellite, *Atmos. Meas. Tech.*, 8, 1575-1591, <https://doi.org/10.5194/amt-8-1575-2015>, 2015.

540 VandenBoer, T. C., Brown, S. S., Murphy, J. G., Keene, W. C., Young, C. J., Pszenny, A., Kim, S., Warneke, C., Gouw, J. A., and Maben, J. R.: Understanding the role of the ground surface in HONO vertical structure: High resolution vertical profiles during NACHTT-11, *J. Geophys. Res. [Atmos.]*, 118, 10155-10171, <https://doi.org/10.1002/jgrd.50721>, 2013.

545 Vogt, E., Held, A., and Klemm, O.: Sources and concentrations of gaseous and particulate reduced nitrogen in the city of Münster (Germany), *Atmos. Environ.*, 39, 7393-7402, <https://doi.org/10.1016/j.atmosenv.2005.09.012>, 2005.

Walker, J., Whittall, D. R., Robarge, W., and Paerl, H. W.: Ambient ammonia and ammonium aerosol across a region of variable ammonia emission density, *Atmos. Environ.*, 38, 1235-1246,

<https://doi.org/10.1016/j.atmosenv.2003.11.027>, 2004.

550 Wang, S., Xing, J., Jang, C., Zhu, Y., Fu, J. S., and Hao, J.: Impact assessment of ammonia emissions on inorganic aerosols in East China using response surface modeling technique, *Environ. Sci. Technol.*, 45, 9293-9300, <https://doi.org/10.1021/es2022347>, 2011.

Wang, S., Nan, J., Shi, C., Fu, Q., Gao, S., Wang, D., Cui, H., Saiz-Lopez, A., and Zhou, B.: Atmospheric ammonia and its impacts on regional air quality over the megacity of Shanghai, China, *Sci. Rep.*, 5, 15842, <https://doi.org/10.1038/srep15842>, 2015.

555 Wang, Y.: MeteInfo: GIS software for meteorological data visualization and analysis, *Meteorological Applications*, 21, 360-368, <https://doi.org/10.1002/met.1345>, 2014.

Wentworth, G. R., Murphy, J. G., Benedict, K. B., Bangs, E. J., and Collett Jr, J. L.: The role of dew as a night-time reservoir and morning source for atmospheric ammonia, *Atmos. Chem. Phys.*, 16, 7435-7449, <https://doi.org/10.5194/acp-16-7435-2016>, 2016.

560 Wiegner, M., Emeis, S., Freudenthaler, V., Heese, B., Junkermann, W., Munkel, C., Schäfer, K., Seefeldner, M., and Vogt, S.: Mixing layer height over Munich, Germany: Variability and comparisons of different methodologies, *J. Geophys. Res. [Atmos.]*, 111, D13201, <https://doi.org/10.1029/2005JD006593>, 2006.

Wu, Y., Gu, B., Erisman, J. W., Reis, S., Fang, Y., Lu, X., and Zhang, X. PM<sub>2.5</sub> pollution is substantially affected by ammonia emissions in China, *Environ. Pollut.*, 218, 86-94, <https://doi.org/10.1016/j.envpol.2016.08.027>, 2016

565 Wu, Z., Hu, M., Shao, K., and Slanina, J.: Acidic gases, NH<sub>3</sub> and secondary inorganic ions in PM10 during summertime in Beijing, China and their relation to air mass history, *Chemosphere*, 76, 1028-1035, <https://doi.org/10.1016/j.chemosphere.2009.04.066>, 2009.

570 Xia, Y., Zhao, Y., and Nielsen, C. P.: Benefits of China's efforts in gaseous pollutant control indicated by the bottom-up emissions and satellite observations 2000–2014, *Atmos. Environ.*, 136, 43-53, <https://doi.org/10.1016/j.atmosenv.2016.04.013>, 2016.

Xu, W., Luo, X., Pan, Y., Zhang, L., Tang, A., Shen, J., Zhang, Y., Li, K., Wu, Q., Yang, D., Zhang, Y., Xue, J., Li, W., Li, Q., Tang, L., Lu, S., Liang, T., Tong, Y., Liu, P., Zhang, Q., Xiong, Z., Shi, X., Wu, L., Shi, W., Tian, K., Zhong,



X., Shi, K., Tang, Q., Zhang, L., Huang, J., He, C., Kuang, F., Zhu, B., Liu, H., Jin, X., Xin, Y., Shi, X., Du, E., Dore, A. J., Tang, S., Collett Jr., J. L., Goulding, K., Sun, Y., Ren, J., Zhang, F., and Liu, X.: Quantifying atmospheric nitrogen deposition through a nationwide monitoring network across China, *Atmos. Chem. Phys.*, 15, 12345-12360, <https://doi.org/10.5194/acp-15-12345-2015>, 2015.

Xu, W., Song, W., Zhang, Y., Liu, X., Zhang, L., Zhao, Y., Liu, D., Tang, A., Yang, D., Wang, D., Wen, Z., Pan, Y., Fowler, D., Collett Jr., J. L., Erisman, J. W., Goulding, K., Li, Y., and Zhang, F.: Air quality improvement in a megacity: implications from 2015 Beijing Parade Blue pollution control actions, *Atmos. Chem. Phys.*, 17, 31-46, <https://doi.org/10.5194/acp-17-31-2017>, 2017.

Yamamoto, N., Kabeya, N., Onodera, M., Takahahi, S., Komori, Y., Nakazuka, E., and Shirai, T.: Seasonal variation of atmospheric ammonia and particulate ammonium concentrations in the urban atmosphere of Yokohama over a 5-year period, *Atmos. Environ.* (1967), 22, 2621-2623, [https://doi.org/10.1016/0004-6981\(88\)90498-2](https://doi.org/10.1016/0004-6981(88)90498-2), 1988.

Yamamoto, N., Nishiura, H., Honjo, T., Ishikawa, Y., and Suzuki, K.: A long-term study of atmospheric ammonia and particulate ammonium concentrations in Yokohama, Japan, *Atmos. Environ.*, 29, 97-103, [https://doi.org/10.1016/1352-2310\(94\)00226-B](https://doi.org/10.1016/1352-2310(94)00226-B), 1995.

Yang, F., Tan, J., Zhao, Q., Du, Z., He, K., Ma, Y., Duan, F., Chen, G., and Zhao, Q.: Characteristics of PM<sub>2.5</sub> speciation in representative megacities and across China, *Atmos. Chem. Phys.*, 11, 5207-5219, <https://doi.org/10.5194/acp-11-5207-2011>, 2011.

Ye, X., Ma, Z., Zhang, J., Du, H., Chen, J., Chen, H., Yang, X., Gao, W., and Geng, F.: Important role of ammonia on haze formation in Shanghai, *Environ. Res. Lett.*, 6, 024019, <https://doi.org/10.1088/1748-9326/6/2/024019>, 2011.

Zbieranowski, A. L., and Aherne, J.: Spatial and temporal concentration of ambient atmospheric ammonia in southern Ontario, Canada, *Atmos. Environ.*, 62, 441-450, <https://doi.org/10.1016/j.atmosenv.2012.08.041>, 2012.

Zhang, L., Wright, L., and Asman, W.: Bi-directional air-surface exchange of atmospheric ammonia: A review of measurements and a development of a big-leaf model for applications in regional-scale air-quality models, *J. Geophys. Res. [Atmos.]*, 115, D20310, <https://doi.org/10.1029/2009JD013589>, 2010.

Zhang, L., Chen, Y., Zhao, Y., Henze, D. K., Zhu, L., Song, Y., Paulot, F., Liu, X., Pan, Y., and Lin, Y.: Agricultural

ammonia emissions in China: reconciling bottom-up and top-down estimates, *Atmos. Chem. Phys.*, 18, 339-355, <https://doi.org/10.5194/acp-18-339-2018>, 2018.

600 Zhang, Q., Streets, D. G., Carmichael, G. R., He, K., Huo, H., Kannari, A., Klimont, Z., Park, I. S., Reddy, S., Fu, J., Chen, D., Duan, L., Lei, Y., Wang, L., and Yao, Z.: Asian emissions in 2006 for the NASA INTEX-B mission, *Atmos. Chem. Phys.*, 9, 5131-5153, <https://doi.org/10.5194/acp-9-5131-2009>, 2009.

Zhang, X., Wu, Y., Liu, X., Reis, S., Jin, J., Dragosits, U., Damme, M. V., Clarisse, L., Whitburn, S., Coheur, P. F., and Gu, B.: Ammonia emissions may be substantially underestimated in China, *Environ. Sci. Technol.*, 51, 12089-12096, <https://doi.org/10.1021/acs.est.7b02171>, 2017.

605 Zhang, Y., Dore, A. J., Ma, L., Liu, X., Ma, W., Cape, J.N., and Zhang, F.: Agricultural ammonia emissions inventory and spatial distribution in the North China Plain. *Environ. Pollut.*, 158, 490-501, <https://doi.org/10.1016/j.envpol.2009.08.033>, 2010.

Zhao, D., and Wang, A.: Estimation of anthropogenic ammonia emissions in Asia, *Atmos. Environ.*, 28, 689-694, [https://doi.org/10.1016/1352-2310\(94\)90045-0](https://doi.org/10.1016/1352-2310(94)90045-0), 1994.

610 Zhao, X., Zhang, X., Xu, X., Xu, J., Meng, W., and Pu, W.: Seasonal and diurnal variations of ambient PM<sub>2.5</sub> concentration in urban and rural environments in Beijing, *Atmos. Environ.*, 43, 2893-2900, <https://doi.org/10.1016/j.atmosenv.2009.03.009>, 2009.

Zheng, G., Duan, F., Su, H., Ma, Y., Cheng, Y., Zheng, B., Zhang, Q., Huang, T., Kimoto, T., Chang, D., Pöschl, U., Cheng, Y., and He, K.: Exploring the severe winter haze in Beijing: the impact of synoptic weather, regional transport and heterogeneous reactions, *Atmos. Chem. Phys.*, 15, 2969-2983, <https://doi.org/10.5194/acp-15-2969-2015>, 2015.

Zhou, Y., Zhu, X., Pan, Y., Tian, S., Liu, Q., Sun, Y., An, J., and Wang, Y.: Vertical distribution of gaseous pollutants in the lower atmospheric boundary layer in urban Beijing, *Environmental Chemistry (in Chinese)*, 36, 1752-1759, 2017.

**Table 1 Overview of measured vertical NH<sub>3</sub> concentration (µg m<sup>-3</sup>) in previous studies and this study.**

Heights (m) / NH <sub>3</sub> (µg m <sup>-3</sup> )	Netherlands		US BAO tower	Beijing IAS tower	
	Rural area	Meteorological tower			
0~5	6.8 (1_m)	8.3	4.7	=	12.5
	6.5 (4_m)				
5~10	-	-	5.0	<u>7.9</u>	13.4
10~20	9.6	-	-	<u>15.8</u>	13.8
20~40	-	6.2	4.61	=	14.2
40~60	-	-	4.19	<u>12.8</u>	14.1
60~80	-	-	-	<u>12.5 (80 m)</u>	<u>14.3 (63 m)</u>
	-	-	-		<u>14.2 (80 m)</u>
80~100	-	3.6	3.6	=	13.9
100~150	-	-	3.09	<u>12.4 (120 m)</u>	14.0 (120_m)
	-	-			13.8 (140_m)
	-	-			13.5 (160_m)
150~200	4.5	2.1	2.72	<u>14.0 (160 m)</u>	13.3 (180_m)
				<u>6.7 (200 m)</u>	12.7 (200_m)
200~250	-	-	2.39	<u>9.1</u>	12.1
250~300	-	-	2.25	<u>7.3</u>	11.8
300~350	-	-	-	<u>7.6</u>	11.3
Period	2014		12/13/2011–1/9/2013	<u>2/10/2009-2/25/2009</u>	3/16/2016–3/16/2017
References	Dammers et al. (2017)	Erisman et al. (1988)	Li et al. (2017)	<u>Zhou et al. (2017)</u>	This study

带格式表格

带格式表格

带格式表格

带格式的：字体颜色：自动设置

带格式的：字体颜色：自动设置

带格式的：字体颜色：自动设置

带格式表格

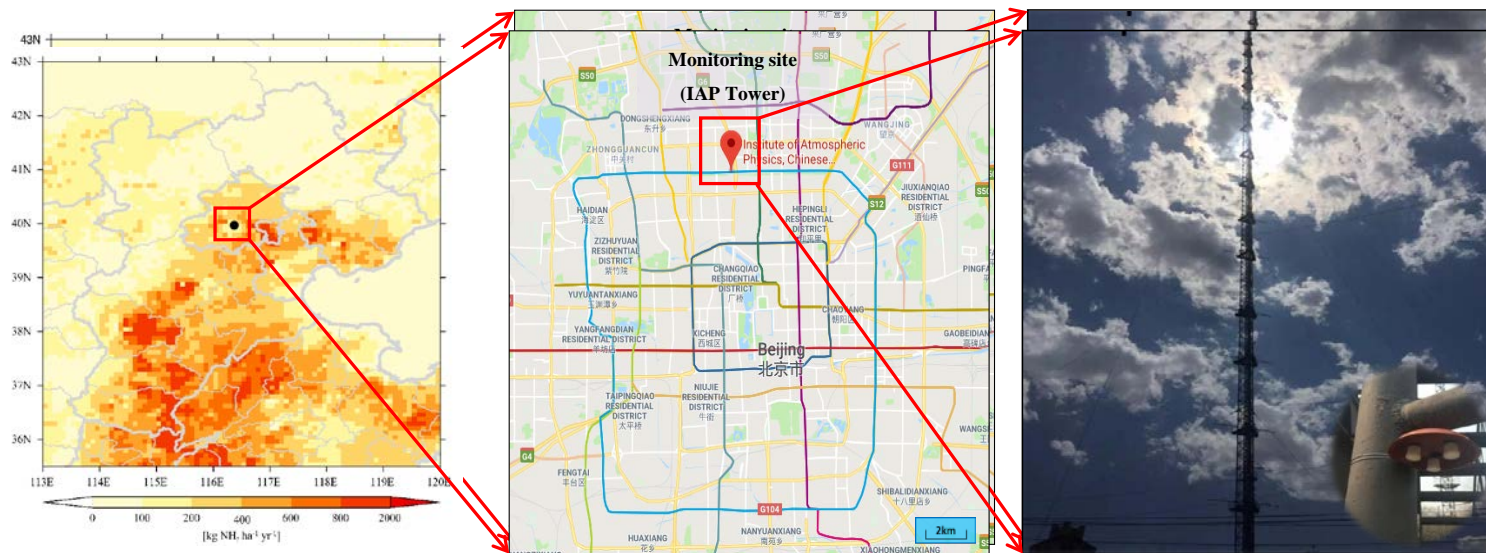


**Fig. 1** Left: Modeled NH<sub>3</sub> emissions distribution (0.1°, ~10 km) over North China Plain in 2015 with the location of the monitoring site shown as a black dot. NH<sub>3</sub> emission estimates are from the inventory of Zhang et al. (2018) at 0.1° horizontal resolution. Right: Map of Beijing showing the location of the monitoring tower.

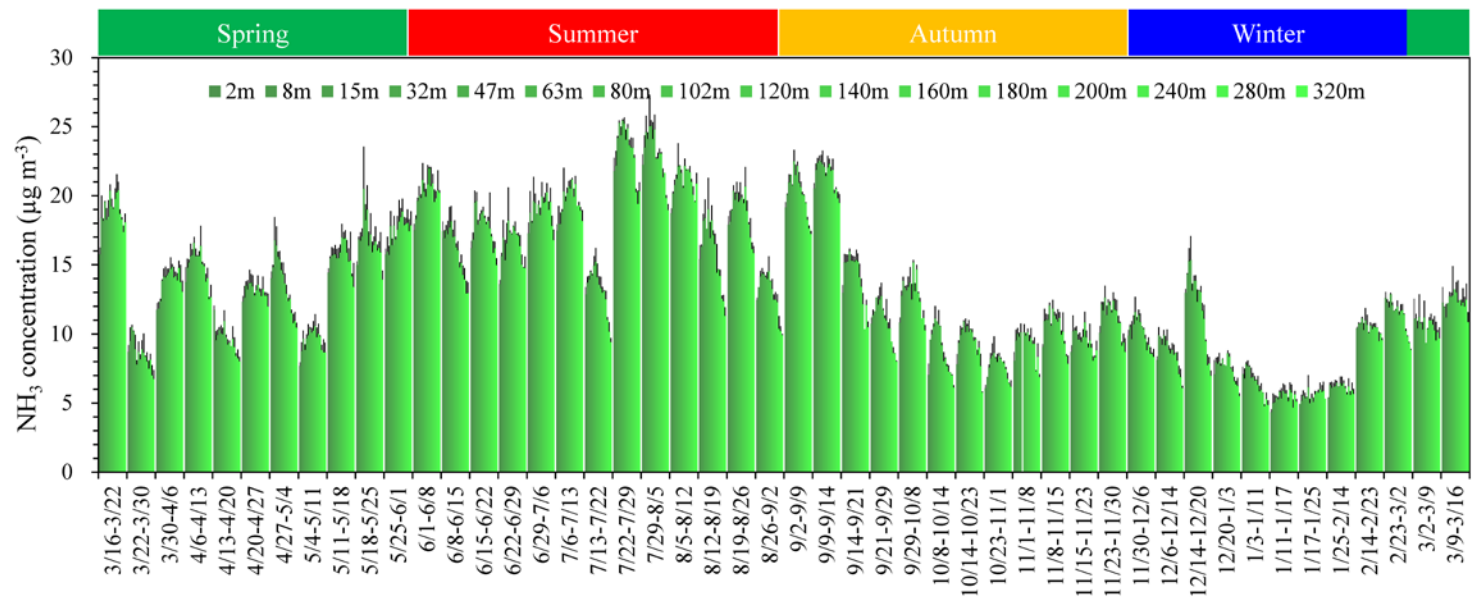
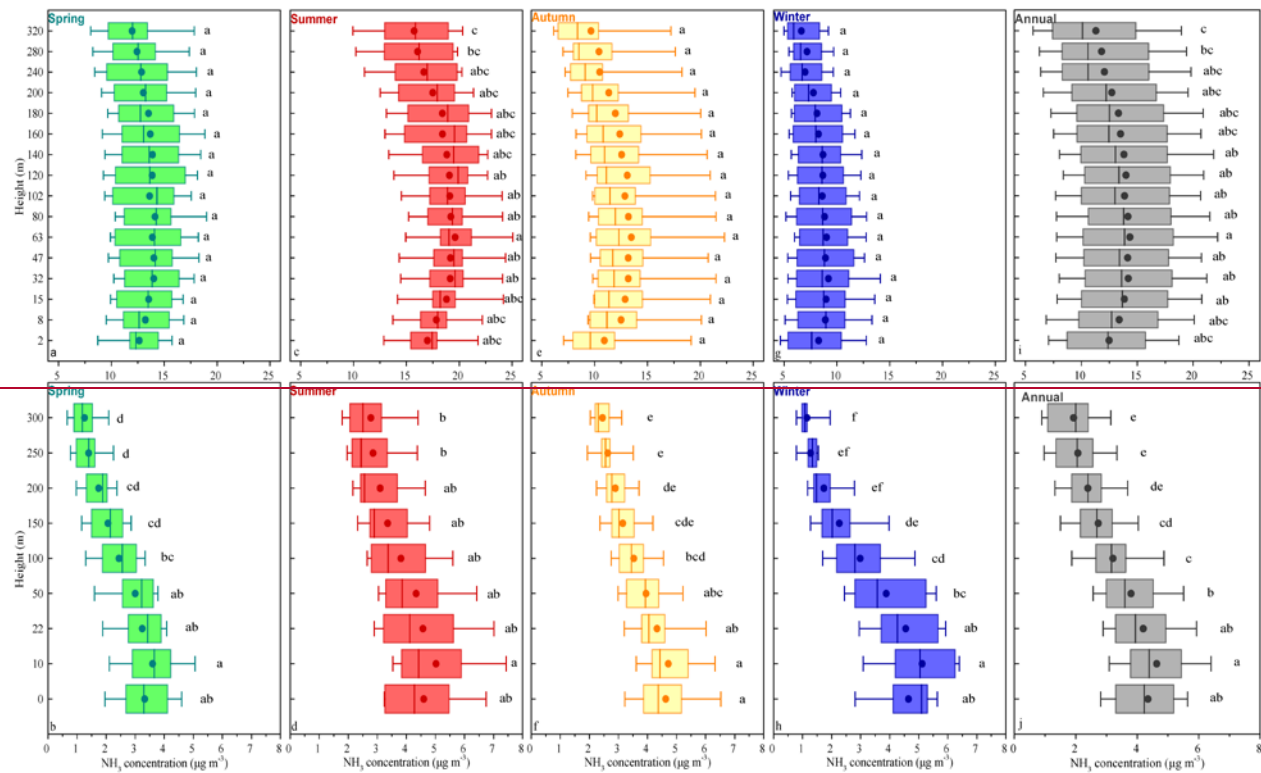


Fig. 2 Time series of vertical distribution of weekly atmospheric NH<sub>3</sub> concentrations ( $\pm\sigma$ ) in Beijing urban (03/16/2016 - 03/16/2017)



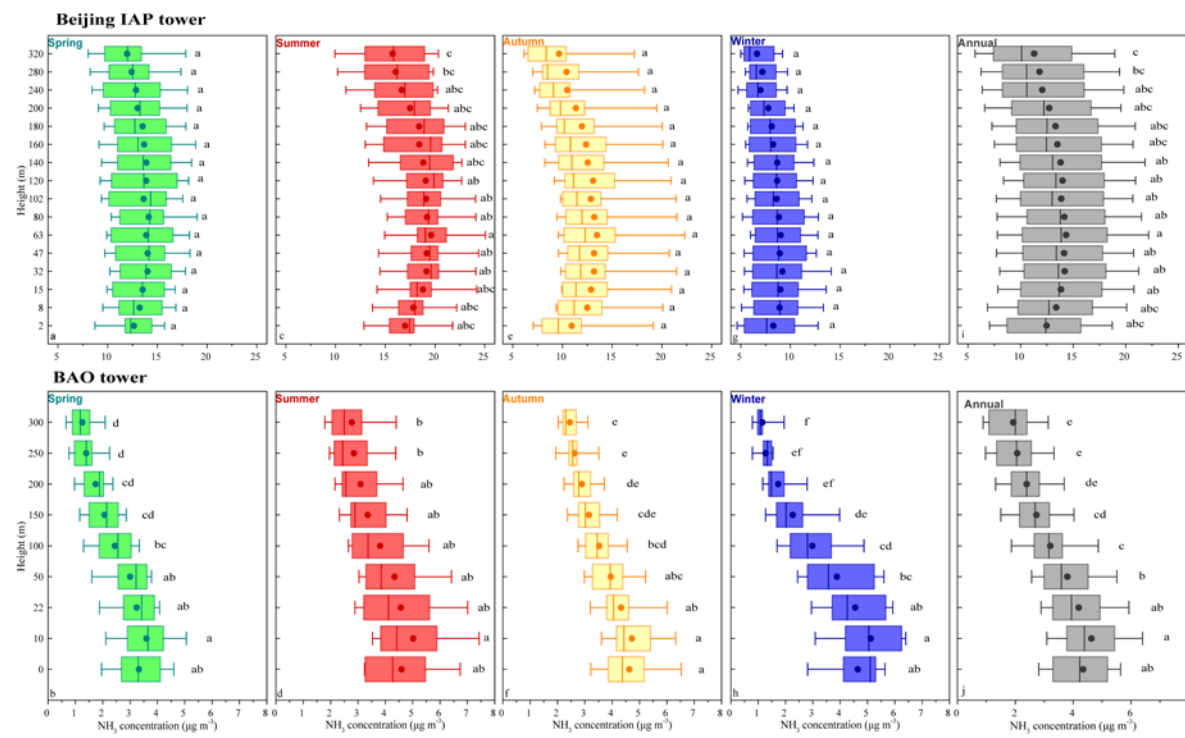
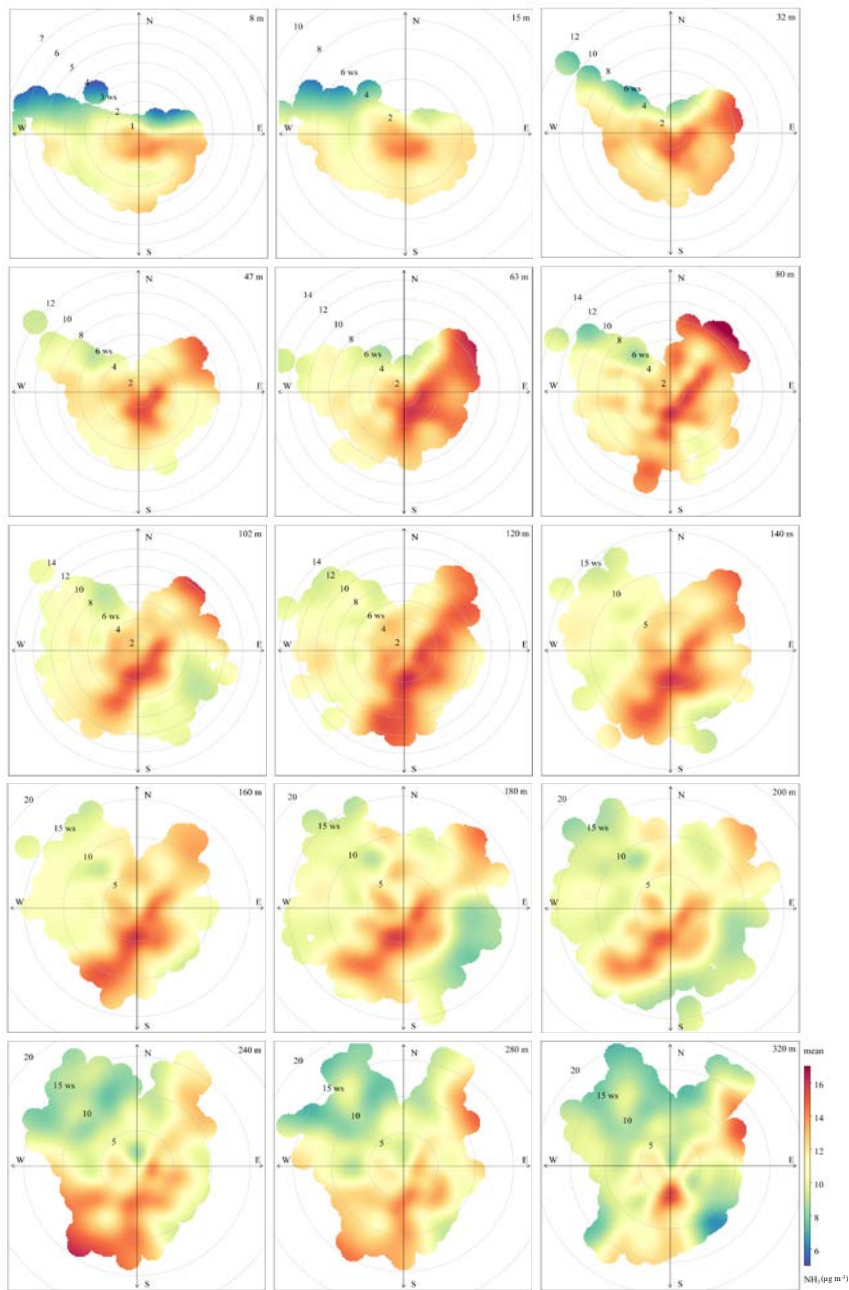
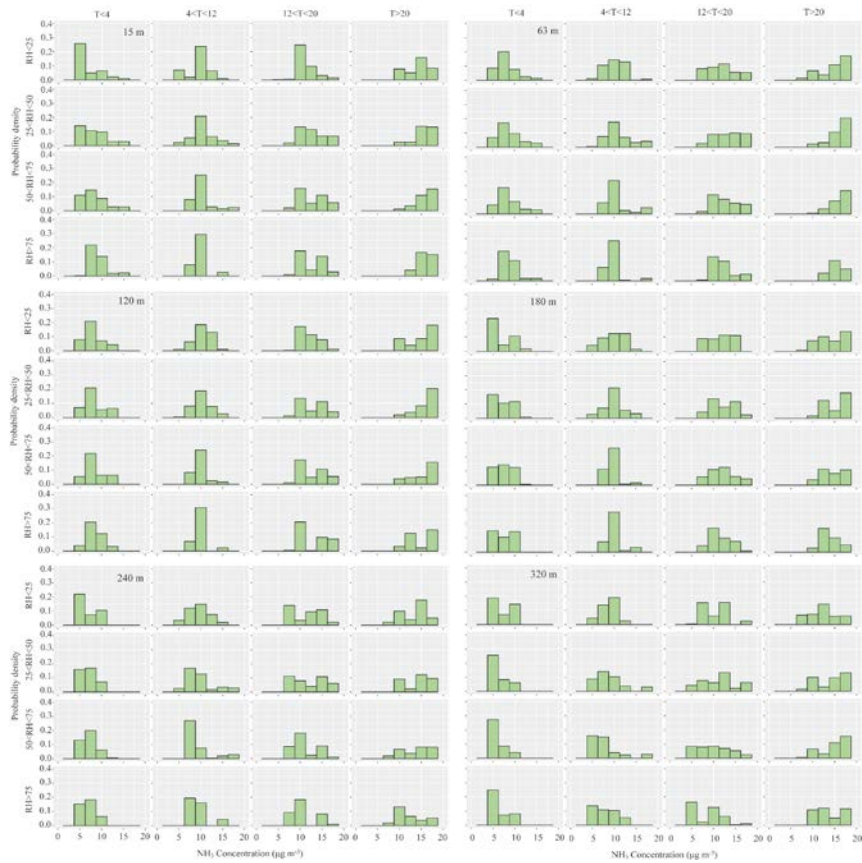


Fig. 3 Comparison of seasonal vertical NH<sub>3</sub> concentrations with the mean (dots), median, 10<sup>th</sup>, 25<sup>th</sup>, 75<sup>th</sup> and 90<sup>th</sup> percentiles of the NH<sub>3</sub> concentrations of each height for IAP tower (Beijing, this study) (fig. a, c, e, g, i) and BAO tower (USA, Li et al., 2017) (fig. b, d, f, h, j).



**Fig. 4** The frequency distributions of wind directions and  $\text{NH}_3$  concentration (color demarcation) for all height during the observation period. Radial data are WS ( $\text{m s}^{-1}$ ) as a function of WD ( $^\circ$ ), The colors denote the  $\text{NH}_3$  concentrations ( $\mu\text{g m}^{-3}$ ).





**Fig. 5** Probability density of NH<sub>3</sub> concentration ( $\mu\text{g m}^{-3}$ ) at different ranges of temperature\* ( $^{\circ}\text{C}$ ) and relative humidity\* (%) for 14 heights.

\* Temperature includes four subsets: <4 $^{\circ}\text{C}$ , 4-12 $^{\circ}\text{C}$ , 12-20 $^{\circ}\text{C}$  and >20 $^{\circ}\text{C}$ ;

\* Relative humidity includes four subsets: <25%, 25-50%, 50-75% and >75%.

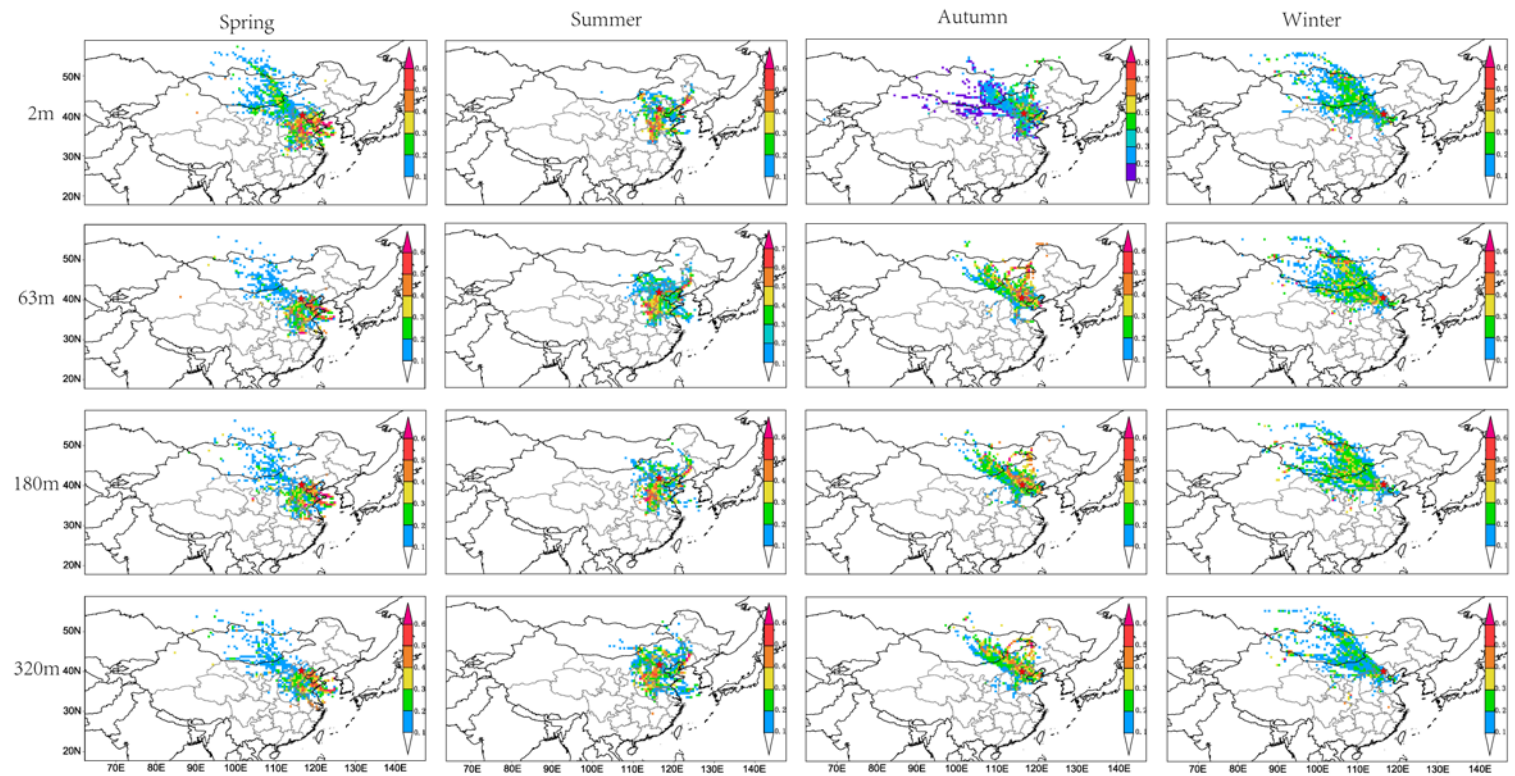


Fig. 6 Weighted potential source contribution analysis (WPSCF) of atmospheric  $\text{NH}_3$  in Beijing during 03/16/2016 – 03/16/2017.